Am J Transl Res 2020;12(4):1203-1221
www.ajtr.org /ISSN:1943-8141/AJTR0102723

Original Article

Effects of tristetraprolin on doxorubicin (adriamycin)-induced experimental kidney injury through inhibiting IL-13/STAT6 signal pathway

Qian Zhang, Ge Wu, Shiyuan Guo, Yong Liu, Zhangsuo Liu

Department of Nephrology, The First Affiliated Hospital of Zhengzhou University, Zhengzhou 450052, Henan, P. R. China

Received September 24, 2019; Accepted March 24, 2020; Epub April 15, 2020; Published April 30, 2020

Abstract: To study the effects of Tristetraprolin (TTP) on Doxorubicin (DOX)-induced experimental kidney injury (KI). DOX was used to induce kidney injury in Balb/c male mice (*in vivo*) and in human kidney proximal tubular epithelial cell line (HK-2) and normal rat kidney epithelial cell line (NRK-52E) (in vitro). Body weight of experimental mice were recorded daily. Histological changes were observed using hematoxylin-eosin (HE) staining, and levels of blood urea nitrogen, serum creatinine and serum cystatin C in KI mice, and MDA, LDH and SOD in cells were detected using the corresponding kits. Meanwhile, the 2, 7-dichlorodihydrofluorescein diacetate (DCF-DA) fluorescent staining was used to assess intracellular levels of reactive oxygen species (ROS). TTP and Kim-1 expressions were measured by immunohistochemistry and western blot. The TNF-α, IL-1β and IL-6 levels were evaluated by ELISA. Expressions of IL-13, STAT6, p-STAT6, Bcl-2, Bax, cleaved-caspase3 were detected using western blot, respectively. Cell Counting Kit-8 (CCK-8) was conducted for analyzing cell viability, and cells apoptosis were assessed by DAPI staining and flow cytometry. DOX treatment decreased body weight and aggravated renal injury without changes in water and food intake. DOX significantly reduced TTP expression, stimulated IL-13/STAT6 pathway and elevated the levels of several factors related to renal injury, including inflammatory response, oxidative stress and cell apoptosis, which were significantly restored by the treatment of overexpression TTP *in vitro*. Overexpression of TTP significantly reduces DOX-induced adverse outcomes so as to prevent renal injury. Inhibition of IL-13/STAT6 pathway may be the functional mechanism under TTP in experimental KI.

Keywords: Nephrotic syndrome, tristetraprolin, doxorubicin, IL-13/STAT6 pathway

Introduction

Nephrotic syndrome (NS), accompaning by kidney injury, is one condition of the primary glomerulonephritis, which is characterized by proteinuria and generalized edema, oxidative stress, chronic inflammation [1]. In the absence of timely prevention and treatment, the final outcome of NS is renal failure. Therefore, it is urgent to seek an effective therapeutic target.

RNA-binding protein tristetraprolin (TTP) is encoded by *Zfp36* gene, and plays a vital role in regulating pro-inflammatory immune responses by destabilizing target mRNAs via binding to their AU-rich elements (AREs) within the 3' untranslated region (3'-UTRs) [2]. When inflammation is activated, TTP expression is alleviated by TTP phosphorylation [3], allowing for the increase in TNF-α mRNAs copies. As a direct consequence of its role as a suppressor of inflammatory signaling, loss of TTP in mice results in the elevated levels of circulating cytokines and chronic inflammation [4]. Most of the characterized suppressor functions of TTP have been associated with its known target genes, including inflammatory cytokines, such as IL-8, IL-6 and IL-23 [5-7]. In glioma, interleukin-13 (IL-13) is involved in cell migration and invasion, which is equipped with ARE in the 3'-UTR, providing the possibility that TTP inhibits its cell invasion and metastasis by degrading IL-13 post-transcriptionally [8]. TTP also suppresses cell growth and induces apoptosis in cell hematopoietic. In leukemia, a striking decrease of TTP induced a sharp increase in

proto-oncogenes, including c-Myc, Bcl-2 and IL-23 [9, 10]. IL-4 could elevate the phosphorylation level of signal transducer and activator of transcription 6 (STAT6), thereby induce TTP expression and inhibit TNF-α production through IL-4/STAT6 pathway in mast cells [11]. When STAT6 is activated and phosphorylated, it is transported from the cytoplasm to the nucleus. In the nucleus, it regulates gene expression in various cell types to mediate many pathologic features of lung inflammatory responses in animal models including Th2 cell differentiation, epithelial mucus production, airway eosinophilia and smooth muscle changes [12]. In pneumonia, IL-4/IL-13 signaling regulates the downstream key protein STAT6 [12, 13]. The IL-13/STAT6 signaling pathway induced mucus hypersecretion and airway inflammation [14]. However, there is rare data about the roles of TTP and IL-13/STAT6 signaling pathway in experimental renal disease.

Doxorubicin (DOX) is composed of a water-insoluble planar tetracycline that binds to the water-soluble sugar daunosamin. DOX may be biotransformed into a free radical, which directly react with oxygen to produce superoxide, causing oxidative stress and ultimately cell death [15]. However, the exact mechanism of DOX-induced toxicity remains unclear. Some researchers hold that the toxicity of DOX was most likely induced by the formation of an iron-anthracycline complex that generates reactive free radicals (ROS) [16, 17]. Previous studies in animals had indicated that DOX caused a renal toxicity and produced progressive glomerular injuries [15]. To study the functions of TTP in the progression of NS, Balb/c mice were treated with DOX as a vivo model, and human kidney proximal tubular epithelial cell (HK-2) and normal rat kidney epithelial cell (NRK-52E) induced with DOX were used as vitro models.

The main aim of the present study was to explore the precise mechanism and exact effects of TTP in DOX-induced NS, excavating methods for ameliorations in an experimental renal disease.

Materials and methods

Animals

Male Balb/c mice (6-8 weeks old; weighing 20-25 g) were purchased from the Laboratory Animal Center of Henan Province (Zhengzhou, China). Mice were raised under standard l aboratory conditions at constant temperature of 24±2°C and relative humidity of 55±5% with a 12 h of light/dark rhythm with free access to water and diet. The present study was approved by the Ethics Committee of The First Affiliated Hospital of Zhengzhou University (Henan, China). All experimental protocols conducted in the mice were strictly followed the Guide for the Care and Use of Laboratory Animals by the National Institutes of Health.

Experimental protocol

Mice were randomly assigned into two groups, control group (n=10) and DOX group (n=10). Mice in DOX group received intraperitoneal (i.p.) injection with a final dose of doxorubicin (5 mg/kg dissolved in 0.9% normal saline) every other day for 2 weeks. Control mice received the same volume of normal saline. Before sacrifice, the body weight of all mice was recorded daily throughout the experimental period (14 days). All mice were then sacrificed under anesthesia with i.p. injection of sodium pentobarbital (50 mg/kg) on day 15.

Blood samples and renal tissues collection

All mice were euthanatized, and blood samples and renal tissues were collected, respectively. Blood samples from the abdominal aorta were then centrifuged at 3500 rpm for 15 min at 4°C and the serum obtained was used for biochemical analysis. Renal tissues were cut into two parts. One part was quickly frozen in liquid nitrogen and stored at -80°C for ELISA and western blot analysis or as a backup, and the other part was fixed in 10% neutral formalin phosphate buffer for HE staining and immunohistochemistry analysis.

Detection of serum biochemical parameters

Blood urea nitrogen (BUN), serum creatinine (Scr) and serum cystatin C (CYS-C) levels in serum of mice were assessed according to instructions of commercial assay kits.

HE staining of renal tissues

The renal tissue samples were fixed in 4% paraformaldehyde buffer (Sigma). Tissue samples

were cleared in xylene and embedded in paraffin after dehydrated in different concentrations of ethanol solution with ascending concentration (70%, 80%, 96%, 100%). The 5-μm thick sections were stained with 0.5% hematoxylin-eosin (HE). The morphological changes in the kidney were blindly assessed under a light microscope (TE2000, Nikon, Japan) (magnification, ×200).

Immunohistochemistry analysis

Similar to HE staining, the tissues were fixed into paraffin and next cut into paraffin-embedded renal sections using a microtome. Tissue sections were then dewaxed, rehydrated and subjected to antigen retrieval in the 0.01 M citrate buffer (pH 6.0). After washing with PBS (0.01 M, pH7.4) twice, the sections were prepared for blocking and incubating with primary antibodies against TTP and Kim-1 overnight and then detected by the biotin-labeled secondary antibody. The bound antibodies were visualized by DAB staining and imaged using a light microscope (TE2000, Nikon, Japan) (magnification, ×200). Brown granules staining in the cytoplasm and/or nucleus represent the positive expression of TTP and Kim-1.

Cell culture and treatment

HK-2 and NRK-52E cells were purchased from the cell bank of Chinese Academy of Sciences (China). Cells were cultured in RPMI 1640 supplemented with 10% fetal bovine serum (FBS, Sigma), 100 U/ml penicillin and 100 μg/ml streptomycin. To mimic nephropathy *in vitro*, HK-2 and NRK-52E cells at 80% confluence were treated with various doses of DOX dissolved in dimethyl sulfoxide (DMSO) (0, 1, 3, 5, 7 and 10 μM) for 24 h. Next, cell viability was assessed after treatment with different doses of DOX to verify the most appropriate DOX dose for the subsequent experiments.

Cell transfection and grouping

According to cell viability, 5 μM of DOX were chosen to induce cells. The overexpression-TTP or negative control (NC) plasmids (Fenghui Biotech, Hunan, China) were transfected into HK-2 and NRK-52E cells using Lipofectamine 2000 (Invitrogen). 24 h after transfection, cells were divided into the following groups, 1) control group, cells were treated with DMSO; 2) DOX group, cells were treated with 5 μM of DOX; 3) overexpression-NC group, cells were transfected with overexpression-NC after treated with 5 μM of DOX; 4) overexpression-TTP, cells were transfected with overexpression-TTP after treated with 5 μM of DOX; 5) overexpression-TTP+IL-13 group, cells were transfected with overexpression-TTP and treated with IL-13 (10 ng/ml) after treated with 5 μM of DOX.

Cell viability assay

The viability of HK-2 and NRK-52E cells was determined using the CCK-8 according to the manufacturer's instructions. Briefly, cells were seeded into 96-well plates with a density of 2.5×10^4 cells/well, and then were predisposed with different concentrations of DOX (0, 1, 3, 5, 7 and 10 μM for 24 h). Additionally, after transfection, cells were incubated for 24, 48, and 72 h. Subsequently, 10 μl of CCK-8 solution was added to the cells for 4 h of incubation at 37°C, and the OD values resulting from CCK-8 staining were measured under a microplate reader at a wavelength (450 nm), which indirectly reflects the viabilities of cells.

Enzyme-linked immunosorbent assay (ELISA)

The levels of TNF-α, IL-1β and IL-6 in mice serums, renal tissue homogenate and cells supernatant were determined by ELISA, using the TNF-α, IL-1β and IL-6 ELISA kits (Shanghai Enzyme-linked Biotechnology Co., Ltd., China) following the manufacturer's instructions. Briefly, samples were placed into the 96-well plates and incubated for 1 h at 37°C with biotin-conjugated antibodies targeting TNF-α, IL-1β and IL-6, followed by culture with enzymatic working solution for 30 min at 37°C. The absorbance at 450 nm were finally detected for quantitation of cytokines levels.

Detection of MDA, LDH and ROS contents and SOD activity

The level of superoxide dismutase (SOD) activity indirectly reflects the ability of the body to scavenge ROS, while the level of malondialdehyde (MDA) indirectly reflects the severity of cells attacked by ROS. The lactate dehydrogenase (LDH) is rapidly released when cell membrane damages, which activity represented the degree of cell damage. HK-2 and NRK-52E cells were collected for preparing cell supernatant

samples. The samples were added to 96-well culture dishes and measured with commercial assay kits for MDA, LDH, ROS and SOD, respectively as described [18].

Detection of intracellular ROS level

The intracellular ROS levels were detected using 2, 7-dichlorodihydrofluorescein diacetate (DCFH-DA) staining. In the presence of ROS, DCFH is oxidized to the enhanced green fluorescent substance DCF that cannot penetrate the cell membrane, and its fluorescence intensity is proportional to the level of intracellular ROS. Briefly, 10 μM of DCF-DA was added into the medium, the HK-2 and NRK-52E cells were incubated for 1 h at 37°C in the dark. After DCF-DA staining, ROS generation in the cells was also observed using a fluorescence microscopy (Olympus) (magnification, ×200).

DAPI staining assay by confocal microscope

After different treatments, the HK-2 and NRK-52E cells in 6-well plates were fixed with 4% formaldehyde at room temperature for 20 min and then stained with DAPI (5 μM) solution. The DAPI-stained cells were observed with a fluorescence microscope (magnification, ×100) for estimation of the percentage of cells not undergoing apoptosis.

Cell apoptosis assay

After different treatments, the HK-2 and NRK-52E cells were cultured until cell confluence reached 80%. Next, cells were seeded into a 6-well plate, and then harvested and washed twice with PBS. Subsequently, Annexin V-FITC (5 μl) and PI (5 μl) were added to the cells and incubated for 10 min at room temperature in the dark, and then cell samples were processed immediately in a BD FACS flow cytometry (BD Biosciences, USA).

Western blot assay

Total protein was extracted from renal tissues, HK-2 or NRK-52E cells using the RIPA lysate and the protein concentration was detected using BCA method. Protein samples (20 μg) were respectively separated on 10% or 12% SDS polyacrylamide gel for electrophoresis, and then electrophoretically transferred onto PVDF membranes. Thereafter, the PVDF membranes were hybridized in blocking buffer overnight at 4°C together with primary antibodies, including TTP (71632; 1:1000; Cell Signaling Technology, Inc.), Kim-1 (ab47635; 1:1000; Abcam), TNF-α (3707; 1:1000; Cell Signaling Technology, Inc.), IL-1β (12242; 1:1000; Cell Signaling Technology, Inc.), IL-6 (12912; 1:1000; Cell Signaling Technology, Inc.), IL-13 (ab106732; 1:1000; Abcam), p-STAT6 (56554; 1:1000; Cell Signaling Technology, Inc.), STAT6 (5397; 1:1000; Cell Signaling Technology, Inc.), cleaved-caspase3 (9661; 1:1000; Cell Signaling Technology, Inc.), caspase3 (9662; 1:1000; Cell Signaling Technology, Inc.), Bax (ab32-503; 1:1,000; Abcam) and Bcl-2 (ab196495; 1:1,000; Abcam). On the next day, the membranes were washed with PBS for 8 mins*5 times; then the membranes were probed by incubation with a secondary antibody for 2 h at room temperature and washed with PBS for 7 mins*6 times before exposure. Finally, the membranes were visualized with ECL chemiluminescence solution and imaged by using a Tanon 4500 System (Tanon, Shanghai, China). All proteins expression were analyzed as described [19] and GAPDH was used as the loading control.

RT-qPCR

Total RNA was isolated from the HK-2 and NRK-52E cells, according to the instructions provided by the manufacturer, using TRIzol reagent (Invitrogen). Subsequently, cDNA was synthesized from RNA (10 μl) through a reverse transcriptase reaction using the First Strand cDNA synthesis kit (Invitrogen). To quantify the relative mRNA expression of TTP (*Zfp36* gene), the primers were synthesized following, forward 5'-GACTGAGCTATGTCGGACCTT-3', and reverse 5'-GAGTTCCGTCTTGTATTTGGGG-3', with GAPDH used as the endogenous control. Real-time PCR was performed using the qPCR SYBR Green Mix (Bio-Rad, Hercules, USA) on an AB 7300 Real time PCR system. Quantitative PCR results were calculated using the $2^{-\Delta\Delta Ct}$ method.

Statistical analysis

Data were presented as the means ± standard deviation (SD) and analyzed using SPSS 13.0 software (IBM). The differences between different groups were analyzed by the one-way analysis of variance (ANOVA), and the differ-

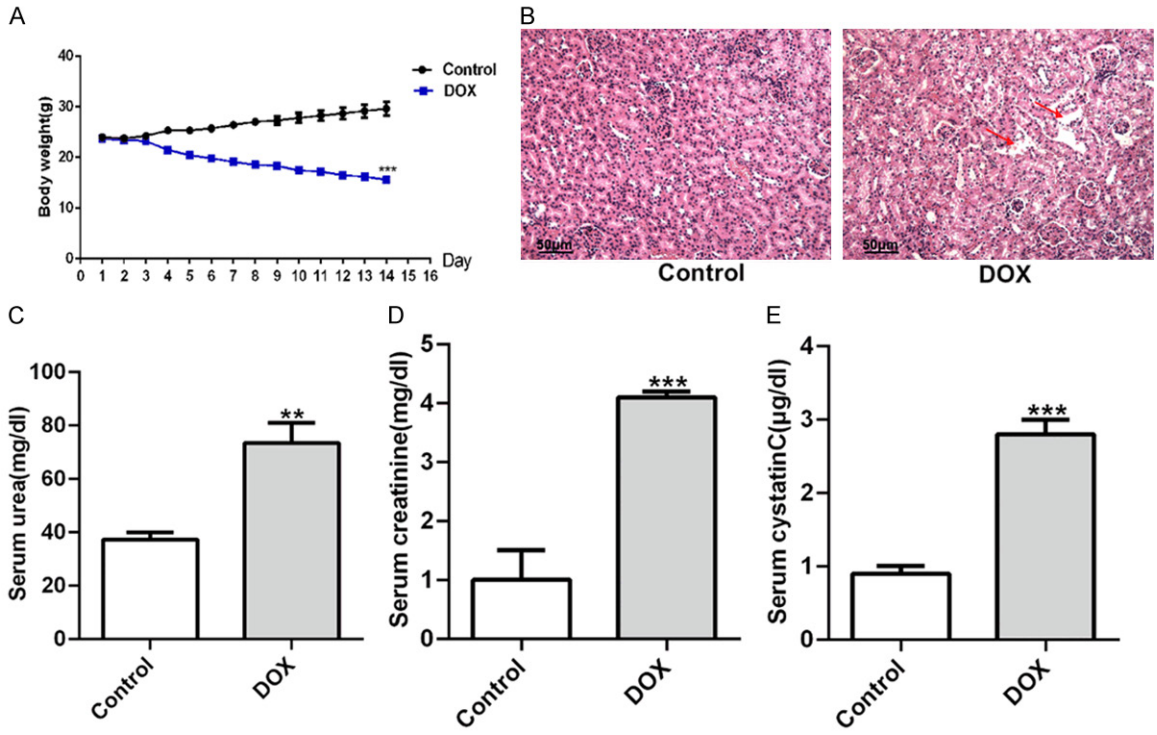

Figure 1. The body weight, morphological changes of renal tissues and serum biochemical parameters in DOX-induced mice. (A) Measurement of body weight daily throughout the experimental period (14 days) in the control and DOX groups. (B) Representative pictures of HE-stained sections of the renal tissues in the control and DOX groups showed the condition of the structures in kidney (200×). The red arrow indicates tissue necrosis and tubular vacuoles. Bar graphs presented the actual measurements of the levels of blood urea nitrogen (BUN) (C), serum creatinine (Scr) (D) and serum cystatin C (CYS-C) (E) in serum in the control and DOX groups. All values were expressed as means ± SD, n=10. **P<0.01 and ***P<0.001 vs. Control.

ences between the two groups were determined using the Student's t-test followed by post hoc Dunnett's test. The correlations between variables were examined using Pearson's correlation coefficient. Differences with P<0.05 were considered statistically significant.

Results

DOX induced the changes of body weight, histological morphology of renal tissue and serum biochemical parameters in DOX mice

Mice in the DOX group lost a significant amount of body weight throughout the experiment, in comparison with control group (**Figure 1A**, P<0.001 at day 14). The **Figure 1B** showed results of histological examination of renal tissues from normal mice and DOX-induced mice. Compared with the control group, section of renal tissue from the DOX group exhibited tubular brush-border loss, interstitial edema, necrosis of epithelium, as well as hyaline casts, tubular vacuoles and protein casts. In addition, serum biochemical parameters were also examined. The serum levels of BUN, Scr and CYS-C were significantly higher in DOX-induced mice than those in the control mice (**Figure 1C-E**, P<0.01 and P<0.001).

The expressions of TTP and Kim-1 in renal tissues

Western blot and immunohistochemically staining demonstrated that DOX induced a significant decrease in TTP expression and a dramatic increase in Kim-1expression in the kidney tissue in comparison to those in the control group (**Figure 2A** and **2B**, P<0.05 and P<0.01). Based on these data, the correlation between TTP and Kim-1 was analyzed using Pearson's correlation coefficient analysis and a significantly negative correlation was found (**Figure 2C**, R^2=0.7907), indicating that TTP might be negatively related to renal injury.

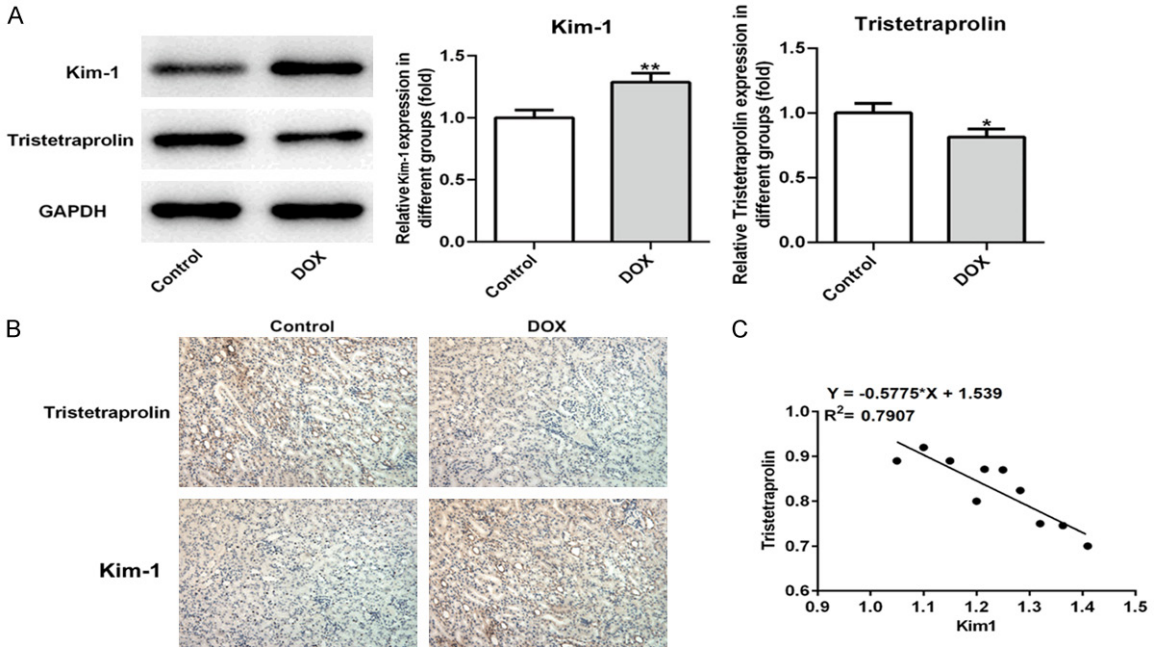

Figure 2. Expressions of Tristetraprolin (TTP) and Kim-1 in DOX-induced mice. A. Western blot analysis for total TTP and Kim-1 and GAPDH in renal tissues. The bar graphs represented the relative expression compared to GAPDH. *P<0.05 and **P<0.01 vs. Control. B. Immunohistochemical staining in the renal tissues of control and DOX groups, showing the TTP and Kim-1 expression (200×). C. Pearson's correlation coefficient analysis demonstrated a significantly negative correlation between TTP and Kim-1. R^2=0.7907. All values were expressed as means ± SD, n=10.

DOX induced an increase in the expression of inflammatory factors and IL-13/STAT6 pathway genes in renal tissue, and serum cytokines containing TNF-α, IL-1β and IL-6

In the renal tissue, the protein expressions of inflammatory factors, including TNF-α, IL-1β and IL-6, were notably increased in the mice predisposed with DOX compared with those in the control mice (**Figure 3A**, P<0.05 and P<0.001). As shown in **Figure 3B**, DOX also significantly enhanced the levels of TNF-α, IL-1β and IL-6 (vs. the control group, P<0.001). In addition, western blot results of IL-13/STAT6 pathway-related proteins in renal tissues were presented in **Figure 3C**. DOX-induced mice had significantly higher protein expressions of IL-13 and p-STAT6 compared to those in control mice (P<0.01 and P<0.001).

Effects of different doses of DOX treatment on the expression of TTP and cell viability in HK-2 and NRK-52E cells

Western blot and RT-qPCR results indicated that different doses of DOX (0, 1, 3, 5, 7 and 10 μM for 24 h) distinctly reduced TTP expression both in HK-2 (**Figure 4A**) and NRK-52E (**Figure 4B**) cells, hinting the inhibitory impact of DOX on TTP in a dose-dependent manner. Similarly, cell viability of HK-2 (**Figure 4C**) and NRK-52E (**Figure 4D**) cells was remarkably weakened after DOX treatment, and this decrease was strengthened with increasing dose. Due to the above finding that cell viability was decreased to near 50% and TTP expression decreased significantly (P<0.001) under DOX treatment at the dose of 5 μM, we chosen DOX at the dose of 5 μM (for 24 h) for subsequent experiments.

Effect of TTP on cell viability

After transfection with overexpression-TTP or overexpression-NC, western blot and RT-qPCR were performed to confirm the transfection efficiency of overexpression-TTP in HK-2 and NRK-52E cell lines. The protein and mRNA expression of TTP in HK-2 and NRK-52E cells was obviously elevated after 24-h overexpression-TTP transfection under DOX treatment (**Figure 5A** and **5B**; P<0.01 and P<0.001). Interestingly, overexpression of TTP could improve the decreased viability of HK-2 and NRK-

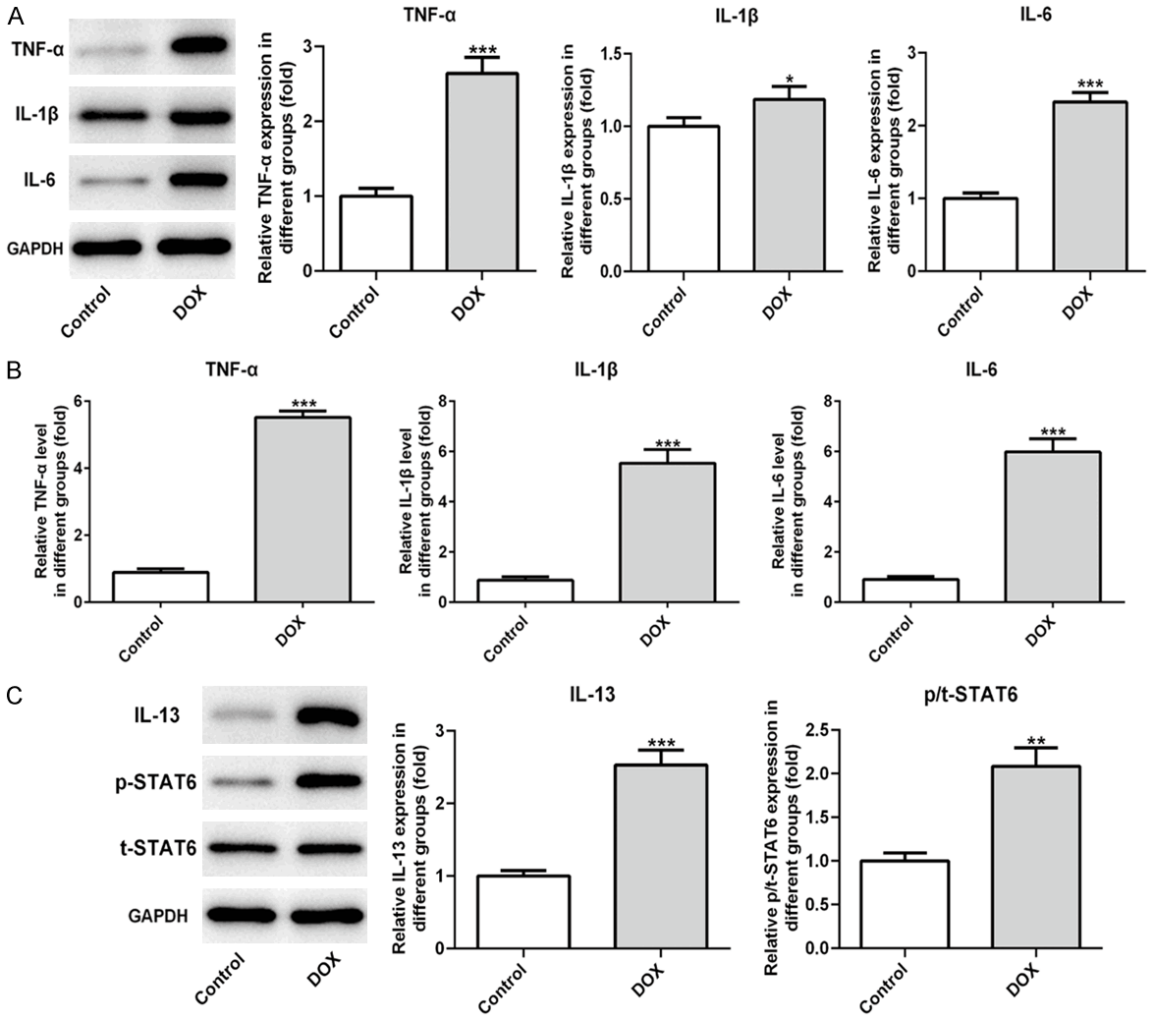

Figure 3. Levels of pro-inflammatory cytokines (TNF-α, IL-1β and IL-6) and IL-13/STAT6 pathway in the renal tissues and serum. A. The protein expression of TNF-α, IL-1β and IL-6 in the renal tissues was determined by western blot. Left part: representative pictures of immunoblots. Right part: densitometric analysis of proteins. B. Serum levels of TNF-α, IL-1β and IL-6 were determined by ELISA kits. C. Western blot for IL-13, phosphorylated (p)-STAT6 and total (t)-STAT6 expression in renal tissues in both control and DOX groups. All values were expressed as means ± SD, n=10. *P<0.05, **P<0.01 and ***P<0.001 vs. Control.

52E cells caused by DOX treatment (**Figure 5C** and **5D**; P<0.01 at 48 h and P<0.001 at 72 h), indicating that existence of TTP was beneficial to cell survival.

Effect of TTP on IL-13/STAT6 signal pathway

Western blot revealed that DOX treatment remarkably increased IL-13 and p-STAT6 expressions in HK-2 and NRK-52E cells, compared with the control cells (**Figure 6A** and **6B**, P<0.001), and TTP overexpression could reduce DOX-promoted IL-13 and p-STAT6 expressions (**Figure 6A** and **6B**; P<0.01 and P<0.001). However, IL-13 and p-STAT6 expressions were up-regulated in in HK-2 cells after addition of IL-13 (10 ng/ml) compared with overexpression-TTP group (**Figure 6A**; P<0.01). Meanwhile, IL-13 treatment raised IL-13 expression (**Figure 6B**; P<0.05) and also induced p-STAT6 expression (**Figure 6B**; P>0.05) in NRK-52E cells compared with overexpression-TTP group. There was no significant differences of total (t)-STAT6 expression under these treatments.

Effects of TTP on pro-inflammatory and oxidative stress

Compared with negative control group, pro-inflammatory factors (TNF-α, IL-1β and IL-6) levels in HK-2 and NRK-52E cells were signifi-

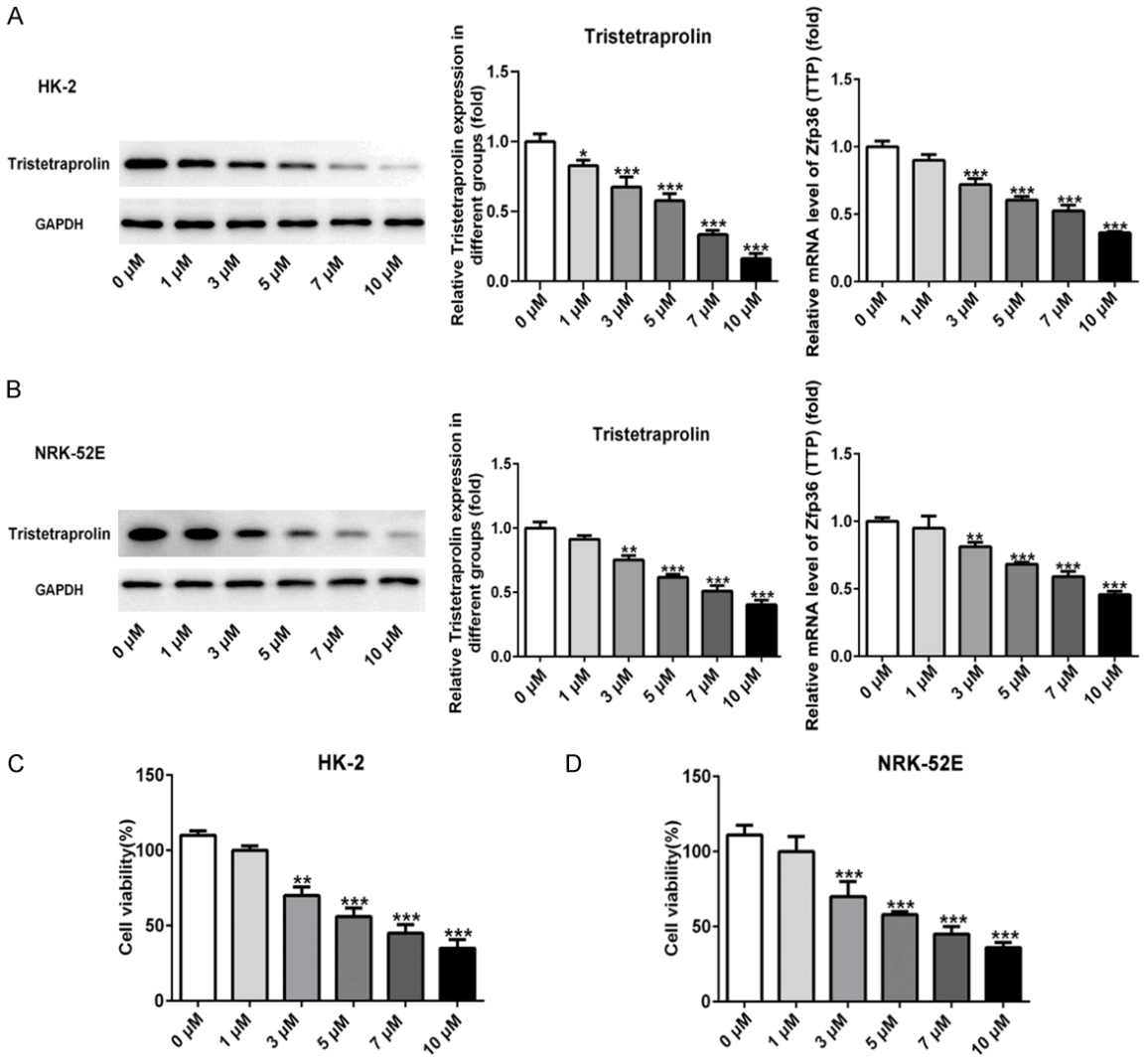

Figure 4. Expressions of Tristetraprolin (TTP) and cell viability in HK-2 and NRK-52E cells after treatment with different doses of DOX. After DOX treatment with various doses (0, 1, 3, 5, 7 and 10 μM), TTP protein expression and mRNA expression in the (A) HK-2 cells and (B) NRK-52E cells were detected using western blot and RT-qPCR, respectively. After DOX treatment at different doses (0, 1, 3, 5, 7, 10 μM), cell viability of (C) HK-2 cells and (D) NRK-52E cells was assessed using CCK-8 assay. All values were expressed as means ± SD, n=5, *P<0.05, **P<0.01 and ***P<0.001 vs. 0 μM.

cantly high in DOX group (**Figure 6C** and **6D**, P<0.001). Besides, TTP overexpression induced obvious decrease in TNF-α, IL-1β and IL-6 levels compared to DOX+overexpression-NC group (**Figure 6C** and **6D**, P<0.001). These changes were reversed when cells were added with IL-13 (P<0.001).

Additionally, DOX-induced group presented distinct elevations in the levels of oxidative stress markers (ROS, MDA and LDH) and a sharp decrease in SOD level in HK-2 and NRK-52E cells compared to control cells (**Figure 7A** and **7B**; P<0.001). Moreover, transfection with overexpression-TTP resulted in significant attenuations of the ROS, MDA and LDH levels (P<0.001) but a significant rise of SOD level (P<0.001) in both HK-2 and NRK-52E cells compared to those in DOX+overexpression-NC group. Subsequently, administration of IL-13 (10 ng/ml) rescued the variations of ROS, MDA, LDH and SOD levels in HK-2 and NRK-52E cells in contrast with overexpression-TTP group (**Figure 7A** and **7B**; P<0.001).

More convincingly, the presence of DCF-DA-positive cells confirmed the formation of ROS in HK-2 and NRK-52E cells with DOX-induced

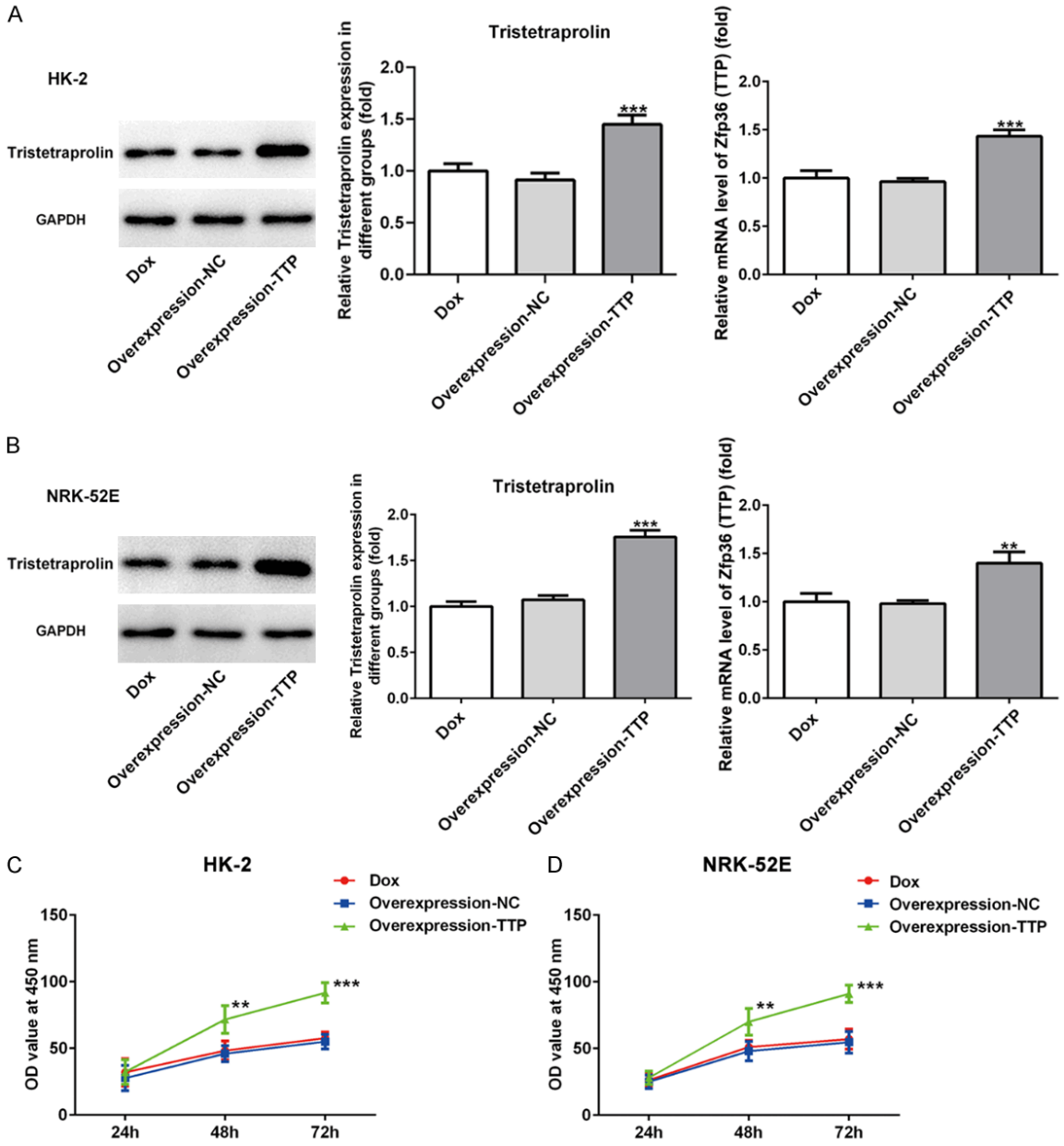

Figure 5. Effect of Tristetraprolin (TTP) on cell viability in HK-2 and NRK-52E cells after treatment with DOX. After transfection of overexpression-TTP, the expressions of TTP protein and mRNA in DOX-treated (A) HK-2 cells and (B) NRK-52E cells were detected by western blot and RT-qPCR, respectively. The cell viability of DOX-treated (C) HK-2 cells and (D) NRK-52E cells was valued by CCK-8 assay after treatment with overexpression-TTP. All values were expressed as means ± SD, n=5, **P<0.01 and ***P<0.001 vs. DOX.

oxidative damage. Treatment with DOX significantly elevated DCF-DA fluorescence in HK-2 (**Figure 7C**) and NRK-52E (**Figure 7D**) cells compared to those in control group. Under treatment with DOX, the DCF-DA fluorescence was significantly lessened through enhancement of TTP. Notably, treatment with IL-13 induced a significant increase in ROS formation (DCF-DA fluorescence) in TTP-overexpressed cells exposed to DOX (**Figure 7C** and **7D**).

Effects of TTP on cell apoptosis and apoptotic markers

After staining with DAPI, the morphology of the nuclei of HK-2 and NRK-52E cells was presented in the **Figure 8A** and **8B**. Chromatin condensation and nuclear fragmentation of cells represented the induction of apoptosis. In the control group, the nuclei were uniformly distributed with normal morphology, but a dra-

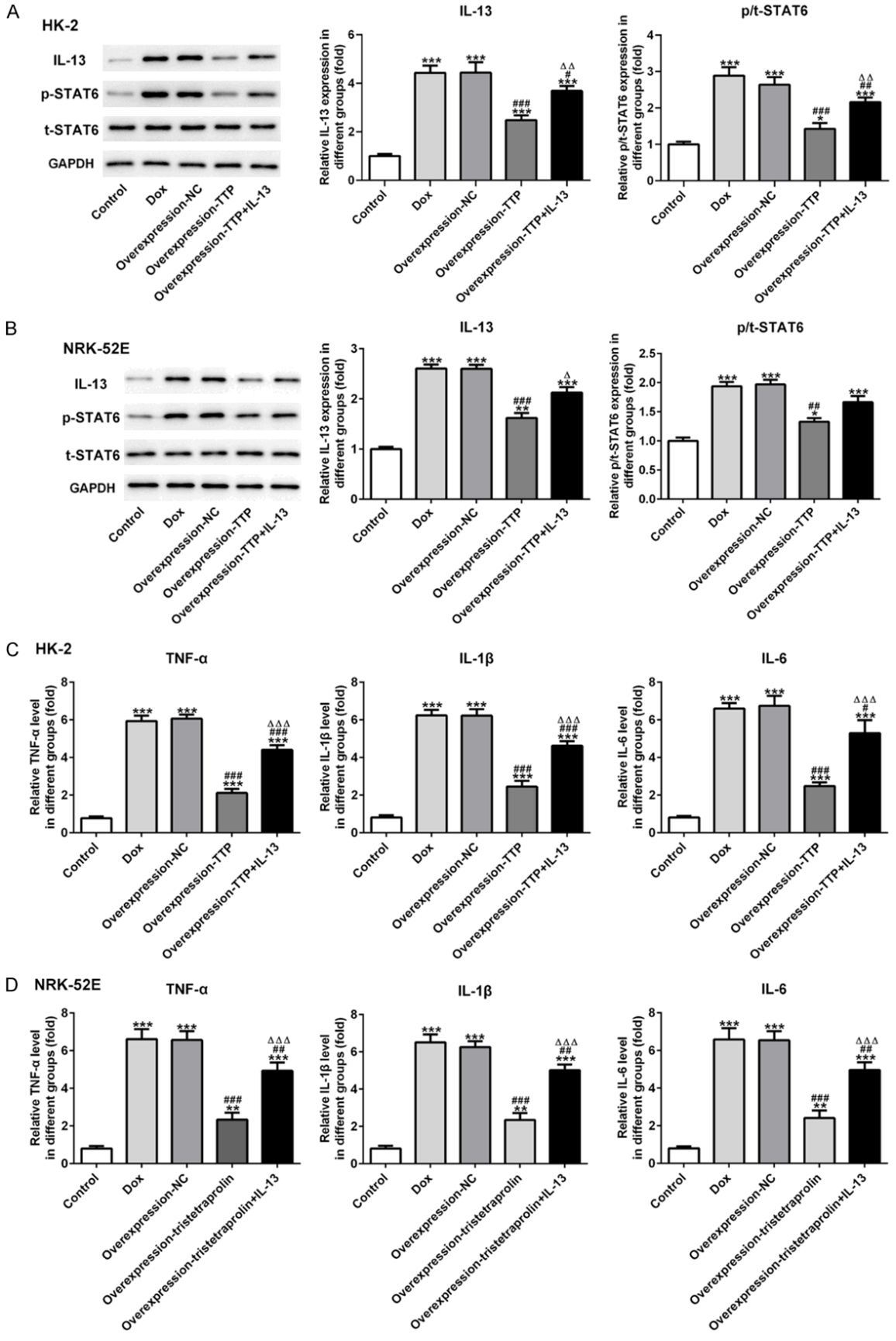
A
HK-2
IL-13
p-STAT6
t-STAT6
GAPDH
IL-13
Relative IL-13 expression in different groups (fold)
p/t-STAT6
Relative p/t-STAT6 expression in different groups (fold)
B
NRK-52E
C
HK-2
TNF-α
Relative TNF-α level in different groups (fold)
IL-1β
Relative IL-1β level in different groups (fold)
IL-6
Relative IL-6 level in different groups (fold)
D
NRK-52E
Control
Dox
Overexpression-NC
Overexpression-TTP
Overexpression-TTP+IL-13
Overexpression-tristetraprolin
Overexpression-tristetraprolin+IL-13

Figure 6. Effects of Tristetraprolin (TTP) on IL-13/STAT6 signaling and inflammation in HK-2 and NRK-52E cells post treatment with DOX. Western blot was carried out in (A) HK-2 and (B) NRK-52E cells of five different groups, showing the IL-13, p-STAT6 and t-STAT6 expressions. ELISA assay was used to measure the levels of TNF-α, IL-1β and IL-6 in (C) HK-2 and (D) NRK-52E cells of the five different groups. All values were expressed as means ± SD, n=5, *P<0.05, **P<0.01 and ***P<0.001 vs. Control; #P<0.05, ##P<0.01 and ###P<0.001 vs. DOX; $^{\Delta}$P<0.05, $^{\Delta\Delta}$P<0.01 and $^{\Delta\Delta\Delta}$P<0.001 vs. Overexpression-TTP.

matic decrease in the number of nucleus (blue dots) appeared in the DOX groups. Fortunately, these were ameliorated to some degree after cells were transfected with overexpression-TTP, suggesting that TTP could alleviate cell apoptosis *in vitro*. However, IL-13 treatment could stimulate cell apoptosis as aforementioned with a decrease in the number of DAPI cyanotic cells both in HK-2 and NRK-52E cells (**Figure 8A** and **8B**).

Meanwhile, the cell apoptosis was measured using flow cytometry by analyzing the percentage of cells in the third quadrant (Q3). As shown in **Figure 8C** (HK-2) and **8D** (NRK-52E), in the control group, the cells were normal, and the apoptosis rate was very small. The apoptosis rate increased significantly after DOX treatment (P<0.001). In contrast, transfection with overexpression-TTP reduced the apoptosis rate noticeably (P<0.001). The apoptosis rate in the overexpression-TTP+IL-13 group also increased when compared with that in the overexpression-TTP group (P<0.001).

In order to determine the anti-apoptotic effect of TTP, the expression of anti-apoptotic protein (Bcl-2) and pro-apoptotic proteins (Bax and Caspase3) were detected in the present study. As shown in **Figure 9A** and **9B**, western blot results revealed that the expression of Bax and Cleaved-caspase3 were increased and the expression of Bcl-2 was decreased significantly in both HK-2 and NRK-52E cells (P<0.001) after treatment with DOX. Meanwhile, overexpression TTP could suppress the increase of Bax and Cleaved-caspase3 and the decrease of Bcl-2 noticeably when compared with DOX+overexpression-NC group (P< 0.01 and P<0.001). Compared with overexpression-TTP group, treatment with IL-13 reduced the expression of Bcl-2 significantly and upregulated the expression of Bax and Cleaved-caspase3 in HK-2 cells (P<0.05, P<0.01 and P<0.001). In addition, IL-13 addition elevated the Bax expression significantly in NRK-52E cells (P<0.05), with no significant effects on the expression of Bcl-2 and Cleaved-caspase3 (P> 0.05) comparing to overexpression-TTP group. However, no statistically significant difference was observed in the caspase3 expression among five groups.

Discussion

A classical NS model [20], with the treatment of DOX, is used in the present study. Administration of DOX caused significant reduction in body weight of mice, which might be due to either decrease food intake or the mobilization and utilization of fat [21]. Also, in the DOX-induced group, the significant increases in BUN, Scr and CYS-C suggested impairment of the kidney function, which coincides with *Alimba et al.*, who has reported that the dramatic increase proteinuria are important for the diagnosis of NS [22]. In the present study, we also found DOX significantly stimulated the production of serum TNF-α, IL-1β and IL-6, and their up-regulated expression in the kidney injury mice. Consistent with our findings, previous studies have shown that Huang Qi Huai (HQH) granules prevent podocyte injury in kidney injury rats by suppressing the pro-inflammatory cytokines, such as IL-1β and TNF-α, etc. [23]. The anti-inflammatory molecule TTP can inhibit the expression of several critical genes involved in the chronic inflammatory diseases and cancers [24]. The kidney injury molecule-1 (Kim-1) is a sensitive and valuable classic biomarker of renal damage [25], and its overexpression is an intermediate step in the sequence of progression from primary tubular activation to end-stage tubulointerstitial damage [26]. Consistent with these studies, in vivo experiments demonstrated a significant elevation of Kim-1 in DOX-treated mice with a striking decrease of TTP compared to normal rats from the western blot quantification and immunohistological localization. Additionally, Kim-1 had a significant negative correlation with TTP. These findings indicated that TTP played a vital role in maintaining the normal morphology of renal tubular cells and retaining normal kidney function.

TTP expression was also significantly decreased in HK-2 and NRK-52E cells after DOX induc-

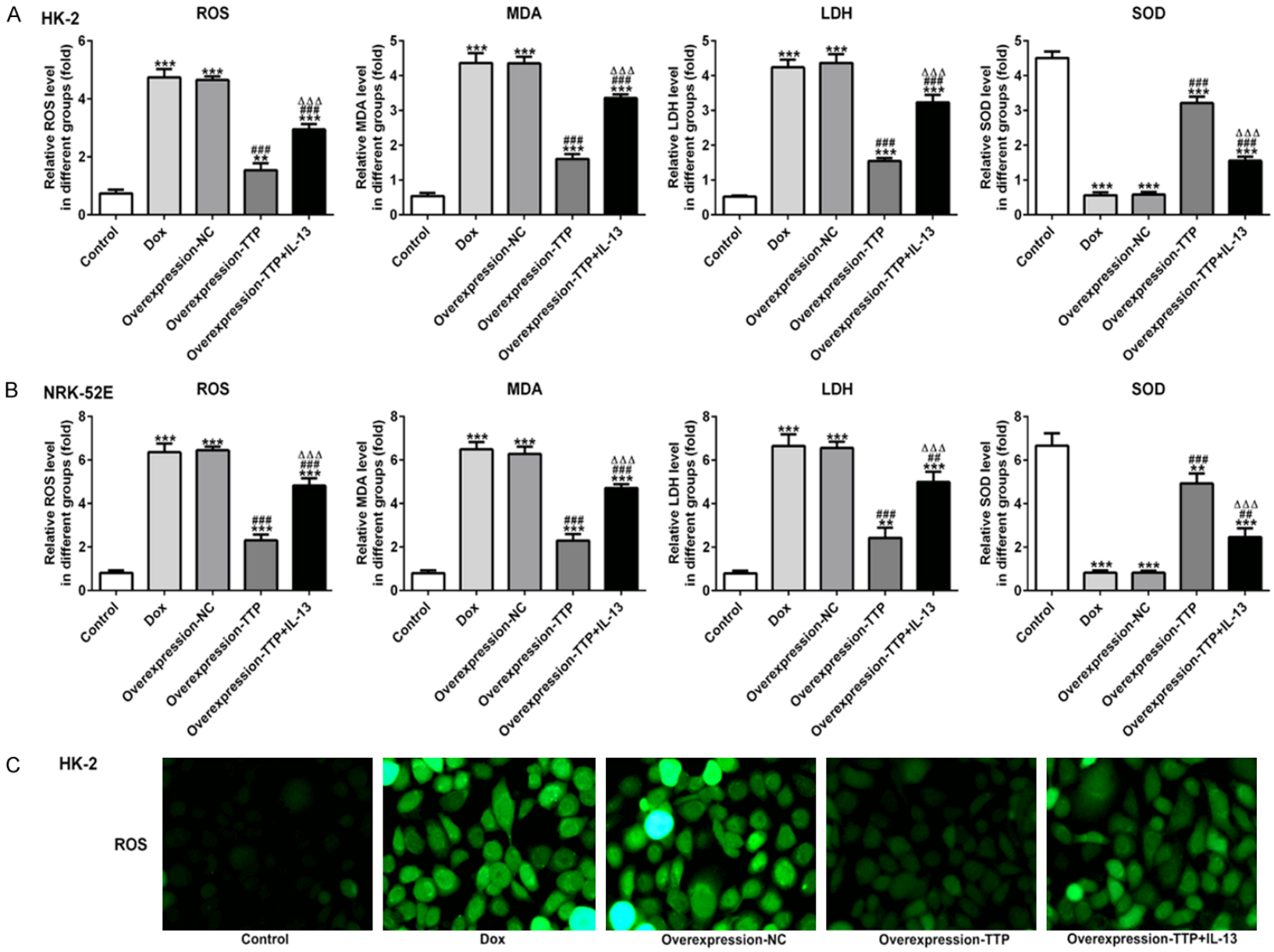
A
HK-2
ROS
MDA
LDH
SOD
Relative ROS level in different groups (fold)
Relative MDA level in different groups (fold)
Relative LDH level in different groups (fold)
Relative SOD level in different groups (fold)
Control
Dox
Overexpression-NC
Overexpression-TTP
Overexpression-TTP+IL-13
B
NRK-52E
ROS
MDA
LDH
SOD
C
HK-2
ROS
Control
Dox
Overexpression-NC
Overexpression-TTP
Overexpression-TTP+IL-13

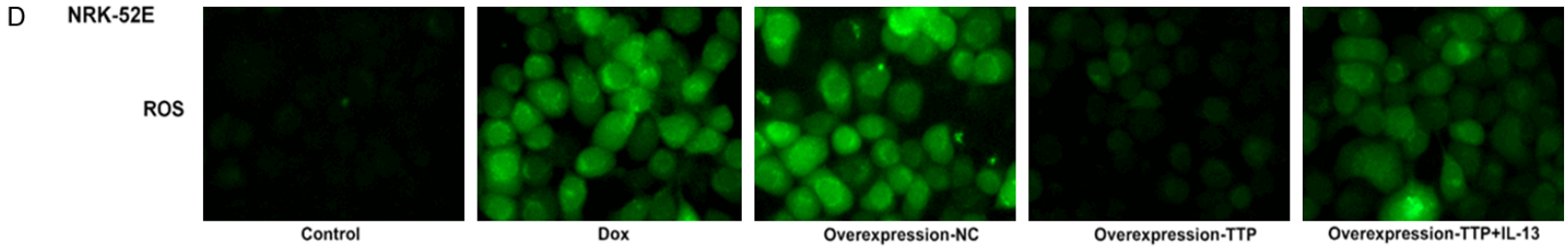

Figure 7. Effect of Tristetraprolin (TTP) on oxidative stress in HK-2 and NRK-52E cells after DOX treatment. (A) The commercial assay kits were conducted to measure the levels of ROS, MDA, LDH and SOD in (A) HK-2 and (B) NRK-52E cells of the five groups. ROS generation was also observed by measuring the DCF-DA fluorescence intensity in (C) HK-2 and (D) NRK-52E cells under a fluorescence microscope at 200× magnification after same treatments as previously described. All values were expressed as means ± SD, n=5, **P<0.01 and ***P<0.001 vs. Control; ##P<0.01 and ###P<0.001 vs. DOX; $^{\Delta\Delta\Delta}$P<0.001 vs. Overexpression-TTP.

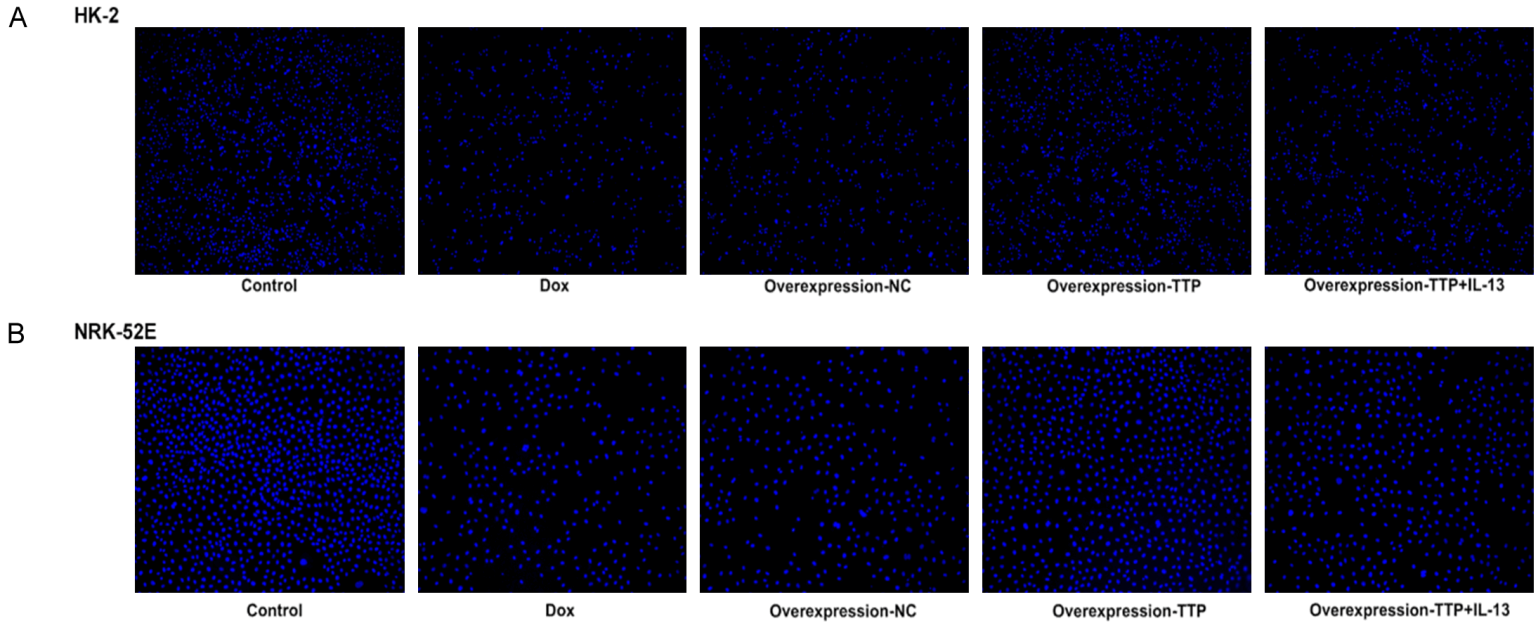

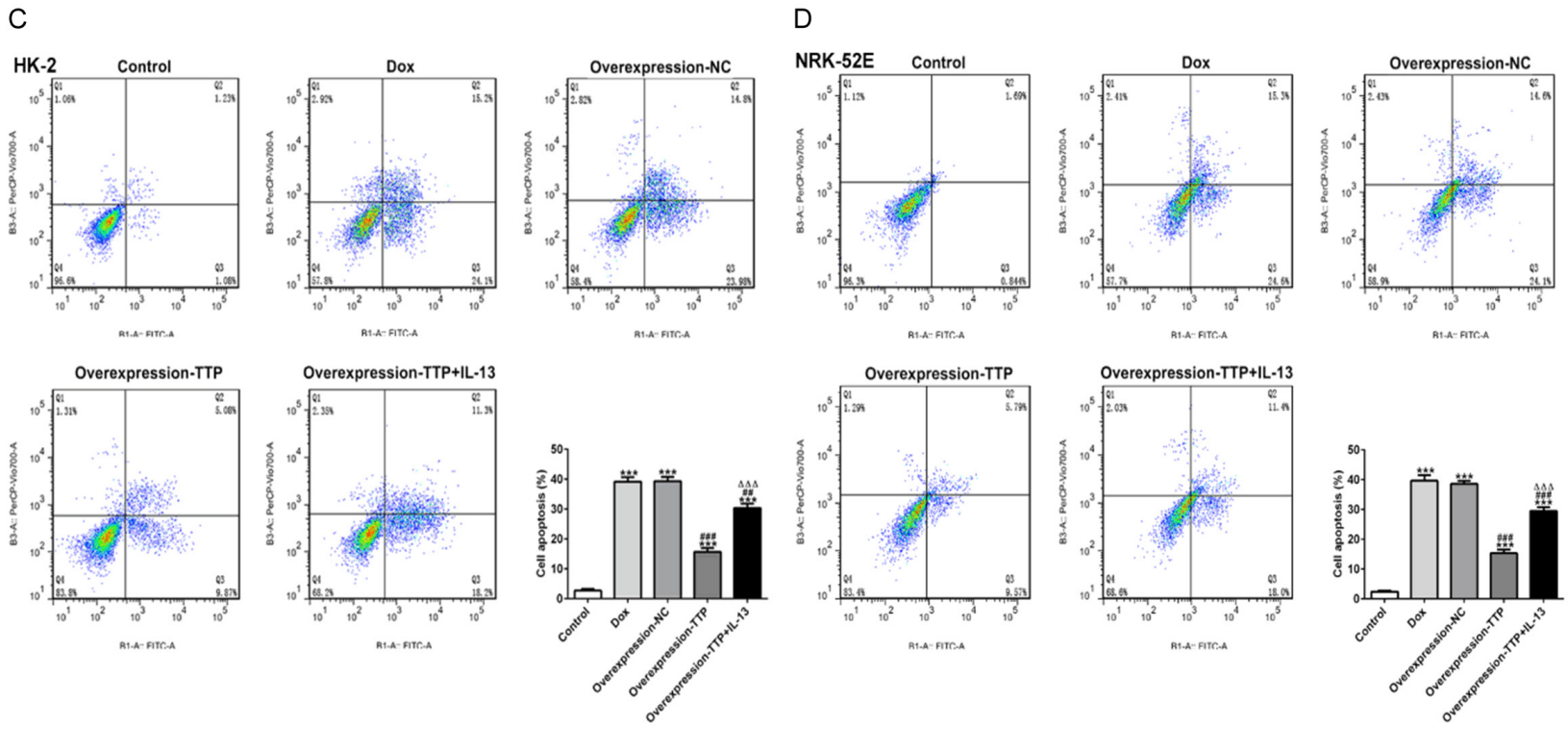

Figure 8. Effect of Tristetraprolin (TTP) on cell apoptosis in HK-2 and NRK-52E cells post DOX treatment. Morphology of (A) HK-2 and (B) NRK-52E cells stained with DAPI typical images were from one of three independent experiments. Cyanotic cells represent living cells (100×). Apoptosis of (C) HK-2 and (D) NRK-52E cells was evaluated by Annexin V-FITC and PI staining using a flow cytometry, and percent of apoptotic cells was quantified. Numbers represent the percentage of the frequency in each quadrant. All values were expressed as means ± SD, n=5, ***P<0.001 vs. Control; ##P<0.01 and ###P<0.001 vs. DOX; $^{\Delta\Delta\Delta}$P<0.001 vs. Overexpression-TTP.

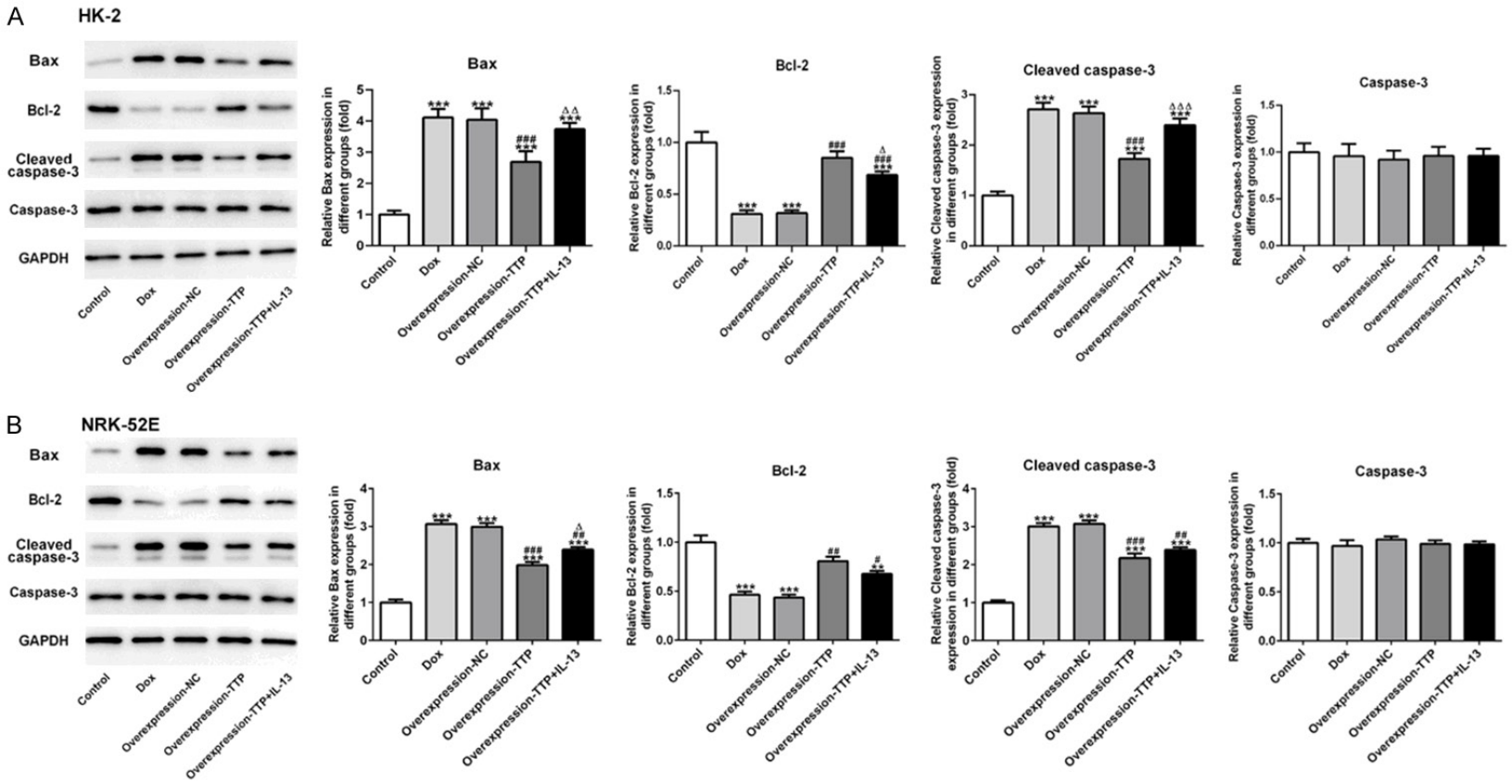

Figure 9. Effect of Tristetraprolin (TTP) on cell apoptosis markers (Bax, Bcl-2 and Caspase-3) in HK-2 and NRK-52E cells after treatment of DOX. Western blot for the detection of Bax, Bcl-2, Cleaved-caspase3, Caspase3 and GAPDH in (A) HK-2 and (B) NRK-52E cells. The bar graphs represented the relative expressions compared to GAPDH. All values were expressed as means ± SD, n=5, **P<0.01 and ***P<0.001 vs. Control; #P<0.05, ##P<0.01 and ###P<0.001 vs. DOX; $^{\Delta}$P<0.05, $^{\Delta\Delta}$P<0.01 and $^{\Delta\Delta\Delta}$P<0.001 vs. Overexpression-TTP.

tion. We used different doses of DOX to stimulate the two cell lines and found that TTP expression gradually decreased with the increase of dose of DOX, and the cell activity also decreased gradually, which also indicated that TTP had a positive effect on maintaining normal cell activity. A relative low dose of DOX dose at 5 μM (above 50% cell viability) was selected for subsequent experiments. Due to the assumption of the positive effect of TTP on cell activity in NS mice, we overexpressed TTP in cell models *in vitro.* In this experiment, TTP overexpression could restore cell viability that was inhibited by DOX induction.

TTP, one of the best characterized RNA-binding proteins, participated in inhibiting the expression of pro-inflammatory cytokines in macrophages. A study had shown that TTP suppressed IL-27 production by targeting the p28 mRNA for degradation, thereby suppressing CD8 T-cell functions [27]. TTP acts as a tumor suppressor by targeting downstream gene IL-13 in the tumorigenesis of glioma [28]. Th2 cytokines, including IL-4, IL-5, IL-10, IL-13, were involved in the onset and progression of NS in minimal change disease (MCNS) [29], and raised level of IL-13 is found in NS and has a role in the pathogenesis of disease [30]. STAT6, a critical transcription factor activated in response to IL-13 [31], becomes phosphorylated at its conserved tyrosine residue Y641, and dimerizes and translocates into the nucleus where it induces the transcription of target genes [32]. The STAT6 mRNA expression was significantly increased and correlated with early unfavorable course of NS in children [33], and STAT6 genes may be associated with predisposition to MCNS [34, 35]. In human epithelial cells from airway, esophagus and intestine, the regulation of eotaxin-3 expression by IL-13 has been shown to require STAT6 activation [36]. IL-13 exposure causes STAT6 activation in up to one third of minimal change disease patients [37]. The above studies suggest that IL-13/STAT6 signaling pathway may play a key role in NS. Similar to these results, we found that the IL-13/STAT6 signaling pathway was activated both *in vivo* and *in vitro*, and that IL-13 promoted STAT6 phosphorylation and nuclear translocation to aggravate kidney injury. What was interesting was that after TTP was overexpressed *in vitro* cell model (both in HK-2 and NRK-52E cells), the IL-13/STAT6 signaling was inhibited, which was restored after IL-13 re-supplementation. These findings firstly indicated that TTP probably negatively regulated the downstream IL-13 signaling pathway and played a protective role in KI.

Inflammation and apoptosis were involved in the pathogenesis of many diseases, such as renal diseases [38]. Meanwhile, we also observed increased expression of pro-inflammatory cytokines (TNF-α, IL-1β and IL-6) both *in vivo* and *in vitro*. After TTP overexpression was administered *in vitro*, decreased pro-inflammatory cytokines and pro-apoptotic factors (Bax and Cleaved-caspase3) were observed, whereas the expression of anti-apoptotic protein (Bcl-2) was increased. However, after IL-13 was added to the cells for activation of the IL-13/STAT6 signaling pathway, the levels of inflammation and cell apoptosis were significantly strengthened, indicating that the IL-13/STAT6 signaling pathway might participate in the regulation of inflammation and apoptosis in kidney injury. The results of DAPI staining and flow cytometry in our study also validated this conclusion.

In the same manner, to explore the antioxidation of TTP in the DOX-induced toxicity in cells, we analyzed the ROS generation, MDA and LDH content, and SOD activity using kits and DCF-DA fluorescent staining. ROS are highly reactive free radicals and induce the oxidative reaction of nucleic acids, proteins and cellular lipids, and cell death due to disruption of the intracellular redox balance [39]. ROS has been postulated to explain the underlying mechanisms of DOX-induced nephropathy [40]. MDA is a typical oxidative marker of the peroxidation of polyunsaturated fatty acids [41] and the LDH release is used to value the integrity of the cell membrane [42]. SOD is known as one of the important enzymatic antioxidant defenses against superoxide radicals [43]. In consistent with these data, we found out enhanced redox state in HK-2 and NRK-52E cells from DOX group in the form of significant increases in ROS, MDA and LDH and a significant depletion in SOD. Overexpression of TTP lowered oxidative stress noticeably, while activation of IL-13/STAT6 signaling could induce excessive ROS accumulation in cells again to cause the oxidative damage.

These findings showed that TTP could alleviate cells injury in DOX-induced KI *in vitro*. We could conclude that the protective mechanism of TTP seemed to be realized through regulating the IL-13/ATAT6 signaling pathway. The limitation of our study lies in the lack of intervention experiments *in vivo* to verify the protective effects of TTP. Based on the conclusion of this study, subsequent experiments will focus on exploring the underlying mechanism of TTP on DOX-induced KI in animals.

This was the first time to reveal that TTP exhibited a significant protective effect against DOX-induced kidney injury, which might be related to the downregulation of the IL-13/STAT6 signaling pathway. Our findings demonstrated that TTP significantly downregulated inflammation, apoptosis and oxidative stress, and suppressed IL-13/STAT6 signaling. Therefore, we hypothesized that TTP probably prevented renal injury via regulating the IL-13/STAT6 signaling pathway. Although more additional studies need to be perform to confirm these findings, the findings in the present study may provide a theoretical foundation for the development of the treatment of NS.

Acknowledgements

The present study was approved by the Ethics Committee of The First Affiliated Hospital of Zhengzhou University (Henan, China).

Disclosure of conflict of interest

None.

Address correspondence to: Dr. Zhangsuo Liu, Department of Nephrology, The First Affiliated Hospital of Zhengzhou University, NO. 1 East Jianshe Road, Zhengzhou 450052, Henan, P. R. China. Tel: +86-037166271067; E-mail: zhsliu2009@126.com

References

[1] Lu R, Zhou J, Liu B, Liang N, He Y, Bai L, Zhang P, Zhong Y, Zhou Y and Zhou J. Paeoniflorin ameliorates adriamycin-induced nephrotic syndrome through the PPARgamma/ANGPTL4 pathway in vivo and vitro. Biomed Pharmacother 2017; 96: 137-147.

[2] Tu Y, Wu X, Yu F, Dang J, Wang J, Wei Y, Cai Z, Zhou Z, Liao W, Li L and Zhang Y. Tristetraprolin specifically regulates the expression and alternative splicing of immune response genes in HeLa cells. BMC Immunol 2019; 20: 13.

[3] Tiedje C, Holtmann H and Gaestel M. The role of mammalian MAPK signaling in regulation of cytokine mRNA stability and translation. J Interferon Cytokine Res 2014; 34: 220-232.

[4] Taylor GA, Carballo E, Lee DM, Lai WS, Thompson MJ, Patel DD, Schenkman DI, Gilkeson GS, Broxmeyer HE, Haynes BF and Blackshear PJ. A pathogenetic role for TNF alpha in the syndrome of cachexia, arthritis, and autoimmunity resulting from tristetraprolin (TTP) deficiency. Immunity 1996; 4: 445-454.

[5] Bourcier C, Griseri P, Grepin R, Bertolotto C, Mazure N and Pages G. Constitutive ERK activity induces downregulation of tristetraprolin, a major protein controlling interleukin8/CXCL8 mRNA stability in melanoma cells. Am J Physiol Cell Physiol 2011; 301: C609-618.

[6] Van Tubergen E, Vander Broek R, Lee J, Wolf G, Carey T, Bradford C, Prince M, Kirkwood KL and D'Silva NJ. Tristetraprolin regulates interleukin-6, which is correlated with tumor progression in patients with head and neck squamous cell carcinoma. Cancer 2011; 117: 2677-2689.

[7] Lee HH, Yang SS, Vo MT, Cho WJ, Lee BJ, Leem SH, Lee SH, Cha HJ and Park JW. Tristetraprolin down-regulates IL-23 expression in colon cancer cells. Mol Cells 2013; 36: 571-576.

[8] Guo J, Qu H, Chen Y and Xia J. The role of RNA-binding protein tristetraprolin in cancer and immunity. Med Oncol 2017; 34: 196.

[9] Rounbehler RJ, Fallahi M, Yang C, Steeves MA, Li W, Doherty JR, Schaub FX, Sanduja S, Dixon DA, Blackshear PJ and Cleveland JL. Tristetraprolin impairs myc-induced lymphoma and abolishes the malignant state. Cell 2012; 150: 563-574.

[10] Molle C, Zhang T, Ysebrant de Lendonck L, Gueydan C, Andrianne M, Sherer F, Van Simaeys G, Blackshear PJ, Leo O and Goriely S. Tristetraprolin regulation of interleukin 23 mRNA stability prevents a spontaneous inflammatory disease. J Exp Med 2013; 210: 1675-1684.

[11] Suzuki K, Nakajima H, Ikeda K, Maezawa Y, Suto A, Takatori H, Saito Y and Iwamoto I. IL-4-Stat6 signaling induces tristetraprolin expression and inhibits TNF-alpha production in mast cells. J Exp Med 2003; 198: 1717-1727.

[12] Walford HH and Doherty TA. STAT6 and lung inflammation. JAKSTAT 2013; 2: e25301.

[13] Liu Y, Zhang H, Ni R, Jia WQ and Wang YY. IL-4R suppresses airway inflammation in bronchial asthma by inhibiting the IL-4/STAT6 pathway. Pulm Pharmacol Ther 2017; 43: 32-38.

[14] Boucherat O, Boczkowski J, Jeannotte L and Delacourt C. Cellular and molecular mecha-

nisms of goblet cell metaplasia in the respiratory airways. Exp Lung Res 2013; 39: 207-216.
[15] Mohamad RH, El-Bastawesy AM, Zekry ZK, Al-Mehdar HA, Al-Said MG, Aly SS, Sharawy SM and El-Merzabani MM. The role of Curcuma longa against doxorubicin (adriamycin)-induced toxicity in rats. J Med Food 2009; 12: 394-402.
[16] DeGraff W, Hahn SM, Mitchell JB and Krishna MC. Free radical modes of cytotoxicity of adriamycin and streptonigrin. Biochem Pharmacol 1994; 48: 1427-1435.
[17] Lee V, Randhawa AK and Singal PK. Adriamycin-induced myocardial dysfunction in vitro is mediated by free radicals. Am J Physiol 1991; 261: H989-995.
[18] Jiang Y, Zhou Z, Meng QT, Sun Q, Su W, Lei S, Xia Z and Xia ZY. Ginsenoside Rb1 treatment attenuates pulmonary inflammatory cytokine release and tissue injury following intestinal ischemia reperfusion injury in mice. Oxid Med Cell Longev 2015; 2015: 843721.
[19] Li H, Yao W, Irwin MG, Wang T, Wang S, Zhang L and Xia Z. Adiponectin ameliorates hyperglycemia-induced cardiac hypertrophy and dysfunction by concomitantly activating Nrf2 and Brg1. Free Radic Biol Med 2015; 84: 311-321.
[20] Barbano B, Gigante A, Amoroso A and Cianci R. Thrombosis in nephrotic syndrome. Semin Thromb Hemost 2013; 39: 469-476.
[21] Boonsanit D, Kanchanapangka S and Buranakarl C. L-carnitine ameliorates doxorubicin-induced nephrotic syndrome in rats. Nephrology (Carlton) 2006; 11: 313-320.
[22] Alimba CG, Dhillon V, Bakare AA and Fenech M. Genotoxicity and cytotoxicity of chromium, copper, manganese and lead, and their mixture in WIL2-NS human B lymphoblastoid cells is enhanced by folate depletion. Mutat Res Genet Toxicol Environ Mutagen 2016; 798-799: 35-47.
[23] Zhu C, Huang S, Ding G, Yuan Y, Chen Q, Pan X, Chen R and Zhang A. Protective effects of Huang Qi Huai granules on adriamycin nephrosis in rats. Pediatr Nephrol 2011; 26: 905-913.
[24] Sanduja S, Blanco FF, Young LE, Kaza V and Dixon DA. The role of tristetraprolin in cancer and inflammation. Front Biosci (Landmark Ed) 2012; 17: 174-188.
[25] Vaidya VS, Ramirez V, Ichimura T, Bobadilla NA and Bonventre JV. Urinary kidney injury molecule-1: a sensitive quantitative biomarker for early detection of kidney tubular injury. Am J Physiol Renal Physiol 2006; 290: F517-529.
[26] van Timmeren MM, Bakker SJ, Vaidya VS, Bailly V, Schuurs TA, Damman J, Stegeman CA, Bonventre JV and van Goor H. Tubular kidney injury molecule-1 in protein-overload nephropathy. Am J Physiol Renal Physiol 2006; 291: F456-464.
[27] Wang Q, Ning H, Peng H, Wei L, Hou R, Hoft DF and Liu J. Tristetraprolin inhibits macrophage IL-27-induced activation of antitumour cytotoxic T cell responses. Nat Commun 2017; 8: 867.
[28] Zeng B, Zhu D, Su Z, Li Z and Yu Z. Tristetraprolin exerts tumor suppressive functions on the tumorigenesis of glioma by targeting IL-13. Int Immunopharmacol 2016; 39: 63-70.
[29] Stangou M, Spartalis M, Daikidou DV, Kouloukourgiotou T, Sampani E, Lambropoulou IT, Pantzaki A, Papagianni A and Efstratiadis G. Impact of Tauh1 and Tauh2 cytokines in the progression of idiopathic nephrotic syndrome due to focal segmental glomerulosclerosis and minimal change disease. J Nephropathol 2017; 6: 187-195.
[30] Mishra OP, Teli AS, Singh U, Abhinay A and Prasad R. Serum immunoglobulin E and interleukin-13 levels in children with idiopathic nephrotic syndrome. J Trop Pediatr 2014; 60: 467-471.
[31] Zhou L, Kawate T, Liu X, Kim YB, Zhao Y, Feng G, Banerji J, Nash H, Whitehurst C, Jindal S, Siddiqui A, Seed B and Wolfe JL. STAT6 phosphorylation inhibitors block eotaxin-3 secretion in bronchial epithelial cells. Bioorg Med Chem 2012; 20: 750-758.
[32] Wang C, Zhu C, Wei F, Zhang L, Mo X, Feng Y, Xu J, Yuan Z, Robertson E and Cai Q. Constitutive activation of interleukin-13/STAT6 contributes to kaposi's sarcoma-associated herpesvirus-related primary effusion lymphoma cell proliferation and survival. J Virol 2015; 89: 10416-10426.
[33] Ostalska-Nowicka D, Smiech M, Jaroniec M, Zaorska K, Zawierucha P, Szaflarski W, Malinska A and Nowicki M. SOCS3 and SOCS5 mRNA expressions may predict initial steroid response in nephrotic syndrome children. Folia Histochem Cytobiol 2011; 49: 719-728.
[34] Kobayashi Y, Arakawa H, Suzuki M, Takizawa T, Tokuyama K and Morikawa A. Polymorphisms of interleukin-4--related genes in Japanese children with minimal change nephrotic syndrome. Am J Kidney Dis 2003; 42: 271-276.
[35] Ikeuchi Y, Kobayashi Y, Arakawa H, Suzuki M, Tamra K and Morikawa A. Polymorphisms in interleukin-4-related genes in patients with minimal change nephrotic syndrome. Pediatr Nephrol 2009; 24: 489-495.
[36] Cheng E, Zhang X, Wilson KS, Wang DH, Park JY, Huo X, Yu C, Zhang Q, Spechler SJ and Souza RF. JAK-STAT6 pathway inhibitors block eotaxin-3 secretion by epithelial cells and fibroblasts from esophageal eosinophilia patients: promising agents to improve inflammation and

prevent fibrosis in EoE. PLoS One 2016; 11: e0157376.
[37] Kim AH, Chung JJ, Akilesh S, Koziell A, Jain S, Hodgin JB, Miller MJ, Stappenbeck TS, Miner JH and Shaw AS. B cell-derived IL-4 acts on podocytes to induce proteinuria and foot process effacement. JCI Insight 2017; 2.
[38] Stambe C, Atkins RC, Tesch GH, Kapoun AM, Hill PA, Schreiner GF and Nikolic-Paterson DJ. Blockade of p38alpha MAPK ameliorates acute inflammatory renal injury in rat anti-GBM glomerulonephritis. J Am Soc Nephrol 2003; 14: 338-351.
[39] Sinha K, Das J, Pal PB and Sil PC. Oxidative stress: the mitochondria-dependent and mitochondria-independent pathways of apoptosis. Arch Toxicol 2013; 87: 1157-1180.
[40] El-Shitany NA, El-Haggar S and El-desoky K. Silymarin prevents adriamycin-induced cardiotoxicity and nephrotoxicity in rats. Food Chem Toxicol 2008; 46: 2422-2428.
[41] Gong K and Li W. Shikonin, a Chinese plant-derived naphthoquinone, induces apoptosis in hepatocellular carcinoma cells through reactive oxygen species: a potential new treatment for hepatocellular carcinoma. Free Radic Biol Med 2011; 51: 2259-2271.
[42] Liu Q, Wang Q, Yang X, Shen X and Zhang B. Differential cytotoxic effects of denitroaristolochic acid II and aristolochic acids on renal epithelial cells. Toxicol Lett 2009; 184: 5-12.
[43] Huang P, Feng L, Oldham EA, Keating MJ and Plunkett W. Superoxide dismutase as a target for the selective killing of cancer cells. Nature 2000; 407: 390-395.